We are IntechOpen, the world's leading publisher of Open Access books Built by scientists, for scientists

4,800
Open access books available

122,000
International authors and editors

135M
Downloads

Our authors are among the

154
Countries delivered to

TOP 1%
most cited scientists

12.2%
Contributors from top 500 universities

CLARIVATE ANALYTICS BOOK CITATION INDEX INDEXED

WEB OF SCIENCE™

Selection of our books indexed in the Book Citation Index in Web of Science™ Core Collection (BKCI)

Interested in publishing with us?
Contact book.department@intechopen.com

Numbers displayed above are based on latest data collected.
For more information visit www.intechopen.com

2

Evapotranspiration Estimation Using Micrometeorological Techniques

Simona Consoli
University of Catania, Department of Agri-food and Environmental Systems Management, Hydraulic Section Catania
Italy

1. Introduction

Accurate evapotranspiration, ET, data are crucial for irrigation management projects, especially in drought prone regions. Evapotranspiration rates can be estimated by micrometeorological methods and the energy balance equation, soil depletion techniques, mass exchange methods, or by using weighting lysimeters. These methods usually are expensive, difficult to operate, and some of them present problems for measurements in heterogeneous vegetation. Therefore, the search for accurate methods for estimating ET fluxes using low-cost, transportable and robust instrumentations is a subject of interest.
The eddy covariance (EC) method is the commonly used micrometeorological technique providing direct measurements of latent heat flux (or evapotranspiration). It adopts a sonic anemometer to measure high-frequency vertical wind speed fluctuations about the mean and an infrared gas analyzer to measure high frequency water concentration fluctuations. These fluctuations are paired to determine the mean covariance of the wind speed and humidity fluctuations about the mean to directly estimate latent heat flux (LE). In the EC method, the sensible heat flux is also estimated using the covariance of the fluctuation in vertical wind speed and variations in temperature about their means. While the preferred method for measuring turbulent fluxes is the eddy covariance (EC) method, the lack of closure is unresolved and a full guidance on experimental set up and raw data processing is still unavailable.
Other energy balance approaches, such as the Bowen ratio and aerodynamic methods, have a sound theoretical basis and can be highly accurate for some surfaces under acceptable conditions.
Biometeorological measurements and theory identified large, organized eddies embedded in turbulent flow, called "coherent structures" as the entities which exchange water vapour, heat, and other scalars between the atmosphere and plant communities.
Based on these studies, a new method for estimating scalar fluxes called "Surface Renewal (SR)" was proposed by Paw U and Brunet (1991). Surface Renewal (SR) theory in conjunction with the analysis of the observed ramp-like patterns in the scalar traces provides an advantageous method for estimating the surface flux density of a scalar. The method was tested with air temperature data recorded over various crop canopies. Results of the studies (Snyder et al., 1996; Spano et al., 1997; Consoli et al., 2006; Castellvì et al., 2008) have demonstrated good SR performance in terms of flux densities estimation, well correlated with EC measurements. The approach has the advantages to (i) require as input

only the measurement of scalar trace; (ii) involve lower costs for the experiment set-up, with respect to the EC method; (iii) operate in either the roughness or inertial sub-layers; (iv) avoid levelling, shadowing and high fetch requirements. Snyder et al. (1996) and Spano et al. (1997), however, have indicated the SR method currently requires an appropriate calibration factor, depending on the surface being measured.
The goal of this chapter is to evaluate the suitability of simple, low-cost methods (i.e. Surface Renewal, aerodynamic methods) to determine sensible heat flux (H) for use with net radiation and soil heat flux density to estimate latent heat flux density or evapotranspiration (LE, or ET). To evaluate the potential for using Surface Renewal analysis to determine H and LE over heterogeneous canopies, high frequency temperature measurements were taken over citrus orchards under semi-arid climatic conditions in Sicily (Italy).

2. Theoretical background

2.1 Energy balance

Biometeorology traditionally depends from the first law of thermodynamics (conservation of energy). In physics, the conservation of energy law says that the "total amount of energy in any isolated system remains constant and can't be recreated, although it may change forms"; for example friction turns kinetic energy into thermal energy.
For a thermodynamic system the first law of thermodynamics may be stated as:

$$\delta Q = dU + \delta W \tag{1}$$

Where δQ is the amount of energy added to the system, δW is the amount of energy lost by the system due to the work done by the system on its surroundings and dU is the increase in the internal energy of the system.
Energy flux can take on several forms. The most obvious energy flux is radiated from all the bodies and absorbed from the sun. Energy may also flow from an object into the ground, and it is called ground heat flux (G). Any object in contact with the air will usually transfer some energy to the air or vice versa, this is called sensible heat flux (H). Evaporation or condensation may occur on a surface, both represent a mass flux to or from the surface. The sign conventions of energy budgets are not completely standardized. Usually the radiation entering a surface is considered positive, and radiation leaving a surface is considered negative. All other energy fluxes have the reverse sign convention. For example sensible heat moving from the air into a surface is considered negative, and sensible heat flux moving from the surface to the air is defined as positive.

$$Rn = LE + H + G + Misc. \tag{2}$$

Where:
- *Rn is the net radiation [W/m²];*
- *LE is the latent heat flux density [W/m²];*
- *H is the sensible heat flux density [W/m²];*
- *G is the soil heat flux density [W/m²];*
- *Misc. is a miscellaneous of flux densities due to the biochemical processes; it's a very small part and generally it can be neglected.*

It's customary to use energy flux densities [W/m²] rather than energy flow [W], so that the analysis of a surface is not specific to the particular surface area being considered.

2.1.1 Sensible heat flux

Heat transfer from a surface to the surrounding atmosphere must take place by either molecular transfer, turbulent transfer, or both processes.

Considering the case of temperature distribution in the air adjacent to a certain surface (Fig. 1). A molecule randomly travels from height (z) to $(z+\ell)$, where (ℓ) is the typical distance that a molecule must travel before it collides with another molecule, transferring its thermal kinetic energy. The molecule is assumed to move with the speed of sound (approximately 300 m s^{-1} near earth's surface). When this molecule from height (z) travels to $(z+\ell)$, it collides and transfers its heat such that a molecule at height $(z+\ell)$ now has the original temperature of the first molecule (temperature expresses the kinetic energy of the molecules).

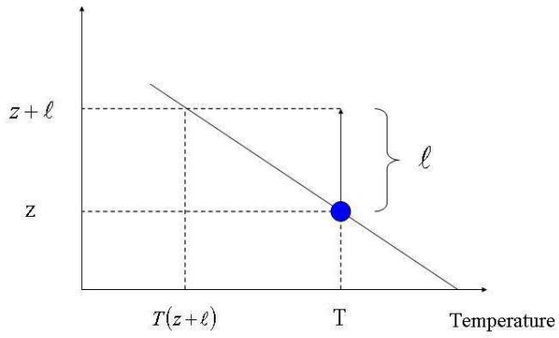

Fig. 1. Mean free path of the air molecule.

The heat transferred per molecule is:

$$h_t = mC_p\left(T_{(z)} - T_{(z+\ell)}\right) \tag{3}$$

Where m is the mass of the molecule and C_p is the specific heat per unit mass.
By using the first-order Taylor approximation:

$$T_{(z+\ell)} = T_{(z)} + \left(\frac{\partial T}{\partial z}\right) + \ell \tag{4}$$

The heat transferred per molecule becomes:

$$mC_p\left(T_{(z)} - \left(T_{(z)} + \frac{\partial T}{\partial z}\ell\right)\right) = -mC_p\frac{\partial T}{\partial z}\ell \tag{5}$$

To find the heat transferred per unit surface area, it's necessary to know the number of molecules per unit area moving away from height (z) to $(z+\ell)$. One may define the number of molecules per unit volume, N. At any time, approximately one-third of the molecules will have components in the z direction; the other two-thirds will have components in the x and y directions. The number density considered active in this process is then N/3.

The flux density F, defined as the number of molecules crossing a unit area perpendicular to z axis in a unit time, is calculated by multiplying N/3 the average speed of the molecules, c:

$$F = \frac{Nc}{3} \tag{6}$$

The heat flux density is the molecular flux density F times the heat carried by each molecule: $-mC_p \frac{\partial T}{\partial z}\ell$:

$$H = -(F)\left(mC_p \frac{\partial T}{\partial z}\ell\right) = -\left(\frac{Nc}{3}\right)\left(mC_p \frac{\partial T}{\partial z}\ell\right) \tag{7}$$

N·m is the mass of a molecule times the number of molecules per unit volume = mass/volume = density (ρ), so eq. (7) becomes:

$$H = \frac{-c\ell}{3}\rho C_p \frac{\partial T}{\partial z} \tag{8}$$

We can define the thermal diffusivity k as $c\ell/3$ [m^2 s^{-1}], thus resulting the equation for sensible heat:

$$H = -k\rho C_p \frac{\partial T}{\partial z} \tag{9}$$

The previous equation for H computation requires the measurement of the gradient of temperature (or concentration) at very small distances from the surface (Stull, 1988).

2.1.2 Latent heat flux

Latent energy caused by evaporation is the major form of cooling for many organisms, including most plants.

The term latent energy flux density describes the energy used in the transfer of water vapour molecules from one phase to another. The energy is used to create a phase change resulting in a mass transfer.

The mass flux of water vapour is needed to determine the latent energy flux. The mass flux density [Kg m^{-2} s] times the energy gained (or lost) per kg of water evaporated, gives the energy flux [J m^{-2} s]. The latent heat of vaporization for water is 2.5 x 10^6 [J kg^{-1}] at 0 °C and decreases to 2.406 x 10^6 [J kg^{-1}] at 40 °C.

It's possible to model the mass flux density of water vapour [kg m^{-2} s^{-1}], "E", in the same manner as for the flux of sensible heat. The gradient theory, derived and based on molecular turbulent transfer is (Stull, 1988):

$$E = -K_w \frac{\partial \rho_v}{\partial z} \tag{10}$$

K_w is the turbulent vapour transport coefficient [m^2 s^{-1}], dependent on stability and turbulent conditions; ρ_v is the absolute humidity [kg m^{-3}]. The absolute humidity is defined as the mass of water vapour per unit volume air.

$$E = \frac{\left[\rho_v(0) - \rho_v(z)\right]}{r_w} \tag{11}$$

where $\rho_v(0)$ is the absolute humidity at the surface and $\rho_v(z)$ is the absolute humidity of the air at height z, r_w is the resistance to water vapour flux [s m^{-1}].
The vapour pressure of water is more used than the specific humidity. The conversion from absolute humidity [kg m^{-3}] to vapour pressure "e" [Pa]:

$$\rho_v = 0.622\frac{e}{P}\rho \tag{12}$$

To obtain the latent energy flux density [J m^{-2} s^{-1}], it is necessary to multiply the evaporative flux density by the latent heat of vaporization, L; e(0) is the vapour pressure of water at the surface, e(z) is the vapour pressure at height z, P is the atmospheric pressure and ρ is the air density [kg m^{-3}] (about 1.2 kg m^{-3}).

$$(L)(E) = \frac{L\rho 0.622}{P}\cdot\frac{\left[e(0)-e(z)\right]}{r_w} \tag{13}$$

If:

$$\gamma \equiv \frac{PC_p}{0.622L} \tag{14}$$

Evaporation from organisms is termed "transpiration", and must be combined with the evaporation term to arrive at the total latent energy transfer from a surface. The combined term for plants is called "Evapotranspiration". For the case of leaves, transpiration takes place in the "sub-stomatal cavity", where vapour pressure "$e_s(T_l)$" is assumed to be saturated at leaf temperature T_l (Stull, 1988).
The resistance term includes two terms, a term for the resistance through the stomata and cuticle "r_s", and a term for the generalized transfer of water vapour through the atmosphere "r_w":

$$LE = \frac{\rho C_p}{\gamma}\frac{\left[e_s(T_l)-e(z)\right]}{\left(r_w+r_s\right)} \tag{15}$$

By expressing the saturated vapour pressure in terms of a first-order Taylor approximation "around" the air temperature:

$$e_s(T_l) \approx e_s\left(T(z)\right) + \Delta\left(T_l - T(z)\right) \tag{16}$$

Where:

$$\Delta \equiv \frac{\partial e}{\partial T} \tag{17}$$

By using the energy budget equation

$$(Rn - G) = H + LE \tag{18}$$

With sensible heat H estimated from the bulk transfer equation:

$$H = \rho C_p \frac{\left(T_l - T(z)\right)}{r_h} \tag{19}$$

r_h is the resistance to heat transfer, also called "aerodynamic resistance". Then:

$$\left(Rn - G\right) - LE = H = \rho C_p \frac{\left(T_l - T(z)\right)}{r_h} \tag{20}$$

$$T_l - T(z) = \frac{r_h}{\rho C_p}\left(Rn - G - LE\right) \tag{21}$$

Finally it's possible to collect the LE terms to obtain the "Penman-Monteith" equation (Allen et al., 1998):

$$LE = \frac{\left(Rn - G\right) + \frac{\rho C_p}{\Delta r_h}\left(e_s\left(T(z)\right) - e(z)\right)}{1 + \frac{\gamma}{\Delta}\frac{r_w + r_s}{r_h}} \tag{22}$$

The Penman-Monteith equation for evapotranspiration is formed by assuming that the stomatal resistance "r_s" is equal to zero. This is true for surfaces that do not have stomatal-type structures that are fully open due to extremely wet conditions. An estimation of evapotranspiration when r_s=0 is called "potential evapotranspiration".

3. Micrometeorological techniques

3.1 Introduction

The surface-atmosphere exchange of scalars (heat, water vapour, carbon dioxide etc.), and vectors (momentum) has been measured and estimated using a variety of techniques. These include eddy-covariance (Swinbank 1955), the eddy-accumulation method (Desjardins, 1972), and gradient/micrometeorological methods (Pruitt, 1963). All of these methods require data logging capable of recording at a range of acceptable frequencies.

In the Eddy Covariance method, high frequency logging (10 Hz or higher) is needed for the 3-D velocity field and the scalar of interest. This, generally, requires sonic anemometer, which is relatively complicated and expensive. The scalar must also be sampled with costly, complex sensors at similar frequencies.

For temperature, however, either the sonic-based temperature (Paw U et al., 2000) or simple, inexpensive temperature sensors such as thermocouples are used. In the eddy accumulation methods, and the relaxed eddy-accumulation, sampling of the scalar is conditionally based on the vertical velocity signal. This reduces the necessity for high-frequency scalar measurements.

In micrometeorological methods, which depend on the measurements of the gradients, such as Bowen Ratio Energy Budget (BREB), advective, or flux-gradient methods, calibrated and carefully matched sensors are needed. In addition, other requirements and limitations exist for each of these methods.

To obtain the sensible heat flux density, the BREB requires measurements of the ground heat flux, biomass storage, and net radiation, and two pairs of high resolution matched

temperature and humidity measurements. Under some conditions, small errors in the matched pair measurements can result in large errors of sensible and latent heat flux density. Also, large errors in latent heat flux density can occur near sunrise and sunset when the Bowen Ratio $\beta = H/\lambda E \approx -1.0$, and the surface is assumed to be horizontally homogeneous, resulting in only vertical transport.

For horizontal and vertical advective-gradient methods several sets of matched sensors pairs are needed. Vertical flux-gradient methods require at least one pair of matched scalar sensors and several wind speed measurements to obtain estimates of the vertical turbulent transport coefficients. Again, horizontal homogeneity is assumed in BREB, and errors in the matched sensors or departures from similarity, may result in potential flux estimation errors.

Tillman (1972) first reported the use of high frequency scalar data (temperature variance data) to determine good estimates of sensible heat flux density (H) under unstable conditions. Weaver (1990) used temperature variance data, similarity theory, and calibration coefficients, that vary depending on the surface and energy balance, to make reasonable estimates of H over semi-arid grass lands and brush under unstable conditions. In 1991 Paw U et al., proposed a new high frequency temperature method (surface renewal) that provides estimates of H regardless of the stability conditions and without the need for temperature profile and wind-speed data. The concept of Surface Renewal was originally developed in the chemical engineering literature, and it is considered an abstraction and simplification of the "transilient" paradigm elucidated by Stull (1984; 1988) for the atmosphere.

3.2 Surface renewal theory

3.2.1 Coherent structures

Coherent structures are characterized by repeated temporal and spatial patterns of the velocity and scalar field. Near a surface, where the fluid is assumed to reach zero velocity, a shear zone must be created if the fluid is moving with respect to the surface. It's theorized that the coherent structures are created by the shear. The atmospheric coherent structures are analogous to those found in theoretical and laboratory flows called "plane mixing layers", defined as flows initially starting out as two distinct layers with different mean speeds, both in parallel directions and in contact with each other at a plane boundary (Paw U et al., 1992). Coherent structures are observed to have ejections and sweeps as common features. In an ejection, the near surface fluid rises upward into the fluid. This is associated with a sweep where fluid farther from the surface descends to the near-surface boundary layer. In an ejection, the fluid has lower horizontal velocity and is moving upward with positive vertical velocity. In a sweep, faster moving fluid descends rapidly in a gust (Stull, 1988).

For flows near typical terrestrial ecosystem, plants frequently have large relatively vertical extent into the atmosphere. The momentum drag created by plant structures slows the air, creating the analogy to plane mixing-layer. When a coherent structure is formed associated with the mean shear near the plant canopy top, it consists of linkage of a sweep with at least one ejection. If the sensible heat flux is positive during the sweep phase, a short-lived rapid horizontal-moving parcel of air gusts into the canopy, bringing cooler air down to the plant elements. In the more quiescent ejection phase, slow horizontal-moving air moves upwards. The ejections are weak near the canopy top (Gao et al. 1989), so the air resides in the canopy sufficiently long to show some heating. This is manifested by a slow temperature rise in the temperature trace with time, and it is terminated by the next gust phase, which causes a sudden temperature drop. The resulting temperature trace exhibits a "ramp" pattern (Gao et al., 1989; Paw U et al. 1992). Under stable conditions, the pattern is reversed, with a slow

temperature drop as the air in the canopy is cooled by the canopy elements, and a sudden temperature rise as a gust brings down the warmer air from above the canopy (Gao et al., 1989; Paw U et al. 1992). Such patterns have been found in the surface layer of the atmosphere and near vegetation also by other researchers and are sometimes associated with gravity (buoyancy) waves.

Van Atta (1977) identified the relationship between structure functions, turbulence and ramp patterns. The structure function, which has been used extensively in turbulence data analysis, is identified as:

$$S^n(r) = \frac{1}{m}\sum_{i=1}^{i=m-j}\left[T(i+j)-T(i)\right]^n \tag{23}$$

Where: m is the number of data points, n is the order of the structure function, j is the sample lag, and i is the data point number. Depending on the sample frequency (f), the sample lag corresponds to a time lag (r) in seconds. For example, if f=8 Hz and j=2, r=2/8=0.25 s.

Van Atta (1977) evidenced that ramps were regular patterns of fixed geometry that had instantaneous terminations for unstable condition, the slow temperature rise would be terminated by an instantaneous temperature drop (Fig. 2a), and for stable conditions, the slow temperature drop would be terminated by an instantaneous temperature rise (Fig 2b). This resulted in a fixed set of probabilities for the structure function values, crucial for the analysis of ramp geometry.

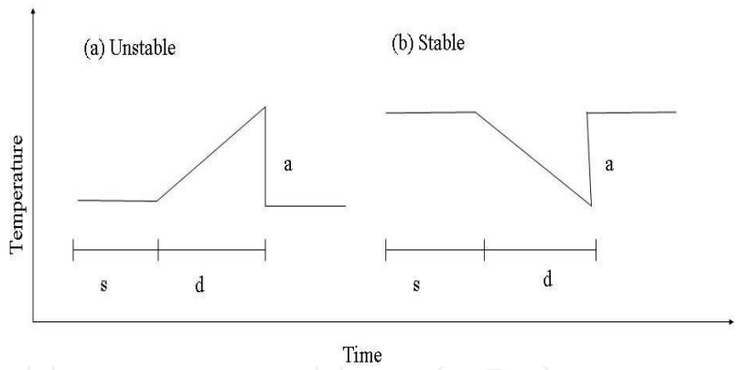

Fig. 2. Hypothetical temperature ramp for (a) unstabe and (b) stable atmospheric conditions

The fixed probabilities are used to determine the ramp dimensions, a, the amplitude of the ramp pattern, s, the spacing between the sudden temperature drop (or rise) and the beginning of the gradual temperature rise (or drop), and, the duration of the gradual temperature rise or fall, d. According to the probability analysis the higher order moments of the structure functions are related to the above ramp dimensions in the following manner:

$$S^2 = \frac{a^2 r}{(d+s)}\left[1-\frac{1}{3}\left(\frac{r}{d}\right)^2\right] \tag{24}$$

$$S^3 = -\frac{a^3 r}{(d+s)}\left[1-\frac{3}{2}\left(\frac{r}{d}\right)+\frac{1}{2}\left(\frac{r}{d}\right)^3\right] \tag{25}$$

$$S^5 = -\frac{a^5 r}{(d+s)}\left[1-\frac{5}{2}\left(\frac{r}{d}\right)+\frac{10}{3}\left(\frac{r}{d}\right)^2-\frac{5}{2}\left(\frac{r}{d}\right)^2-\frac{2}{3}\left(\frac{r}{d}\right)^5\right] \tag{26}$$

It's possible determine the ramp dimensions d and s by using more than one time lag, and then solutions, assuming r<d and r<s:

$$\frac{S^3(br)}{S^3(r)} = \frac{-\frac{a^3 br}{(d+s)}\left[1-\frac{3}{2}\left(b\frac{r}{d}\right)+\frac{1}{2}\left(b\frac{r}{d}\right)^3\right]}{-\frac{a^3 r}{(d+s)}\left[1-\frac{3}{2}\left(\frac{r}{d}\right)+\frac{1}{2}\left(\frac{r}{d}\right)^3\right]} \equiv R \tag{27}$$

If $v \equiv \frac{r}{d}$ and $v^3 - \frac{12-3R}{16-R}v + \frac{4-2R}{16-R} = 0$

which yields a cubic solution for v and therefore d. The ramp amplitude can be obtained from

$$a^3 + \left[10S^2(r) - \frac{S^5(r)}{S^3(r)}\right]\frac{P_3}{P_5}a + 10S^3(r)\frac{P_3}{P_5} = 0 \tag{28}$$

Where: $P_2 = 1-\frac{1}{3}v^2$; $P_3 = 1-\frac{3}{2}v+\frac{1}{2}v^3$; $P_5 = 1-\frac{5}{2}v+\frac{10}{3}v^2-\frac{5}{2}v^3+\frac{2}{3}v^5$

And s is given by

$$s = \frac{-a^3 r}{S^3(r)}P_3 - d \tag{29}$$

Chen et al. (1997) noted that the ramps observed by Gao et al. (1989) and Paw U et al. (1992) had non-instantaneous terminations. They developed a set of equations to obtain the ramp dimensions, with the assumption that the spacing between ramps (s) was zero.

Surface Renewal (SR) analysis, as used in plant canopies, was originally conceived of as a simple "transilient" theory (Stull, 1984) in a pseudo-Lagrangian sense (Paw U et al. 1995). In SR only two heights are considered, some height above a plant canopy, and a height representing the entire plant canopy. The vertical motions are not followed. In figure 3 we may consider an air parcel, which instantaneously moves down and then it travels horizontally.

Parcel instantly drops from position 1 to position 2 in the canopy (upper cartoon). Canopy is a source of scalar, time goes on but the scalar does not increase because there is a speed of diffusion of the scalar (thermal inertia) (position 2 to 3 in the lower chart). Scalar starts to increase in the parcel (position 3, 4) to a peak (positions 5, 6 in the lower chart). After horizontally advecting some distance, the parcel instantly rises from position 5 to 6 in the upper cartoon. Simultaneously, from position 7, a new parcel instantly replaces the old parcel's position in the canopy, shown as position 8 (offset horizontally in the upper cartoon

for clarity). This results in an instantly falling of the scalar value (lower graph), terminating the previous gradual scalar increase and forming the ramp pattern.

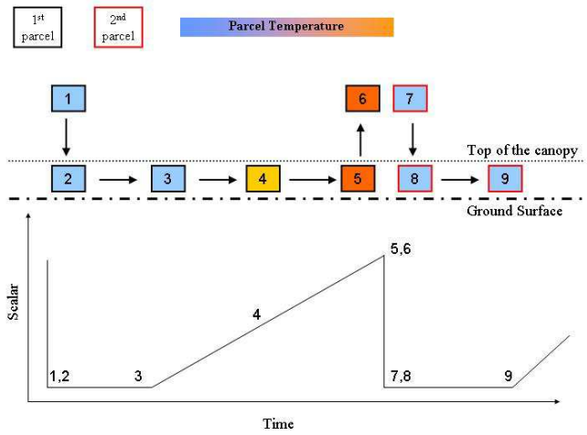

Fig. 3. Example of Surface Renewal process

3.2.2 Calibration

Under unstable conditions, (Fig. 3), a ramp will be determined by the warming caused by the plant canopy elements. In Paw U et al. (1995), the sensible heat flux density within a coherent structure, was derived as:

$$H' = \rho C_p \frac{dT}{dt}\left(\frac{V}{A}\right) \tag{30}$$

Where $\left(V/A\right)$ is the ratio of the volume over the horizontal area of the parcel (for a parcel in the canopy, this would be the canopy height). Practically for temperature recorded at the canopy top, the surface renewal equation is expressed as:

$$H = \alpha \rho C_p \frac{dT}{dt} h_c \tag{31}$$

Where T is measured at the canopy heigh, h_c is the canopy heigh and α is a calibration factor embodying temperature variation in the canopy, initially estimated at 0.5 to account for linear change in temperature with height. The time derivative represents the heating during the time period of the ramp, and during the spacing between ramps, when no heating occurs. Any advection or other processes not properly described in surface renewal analysis would also be included in α (Paw U et al. 1995). When the ramp dimensions are determined by structure functions, then the following equation for H is used to define the sensible heat flux density during a ramp:

$$H = \alpha \rho C_p \frac{dT}{dt} h_c \approx \alpha \rho C_p \frac{\partial T}{\partial t} h_c = \alpha \rho C_p \frac{a}{d} h_c \tag{32}$$

When the equation is weighted by the fraction of time during the ramp $\frac{d}{d+s}$, then the sensible heat flux density may be written as:

$$H = \alpha\rho C_p \frac{a}{d} h_c \left[\frac{d}{d+s} \right] = \alpha\rho C_p \frac{a}{d+s} h_c \tag{33}$$

Uncalibrated SR sensible heat flux density provides an estimate of H that is uncorrected for the mean parcel size, the unequal heating of air from the ground to the thermocouples, and micro-scale advection effects. When sensible heat flux density (H) from a sonic anemometer is plotted versus uncalibrated SR H', a good correlation is typically observed, the slope of the regression line through the origin is the α calibration factor.

It's possible to process the high frequency temperature data to obtain half hour means of the 2nd, 3rd, and 5th order moments of the time lag temperature differences (Snyder et al., 2000). The obtained moments are, then, used to determine the ramp amplitude (*a*) and inverse ramp frequency (*d*+*s*) using Van Atta (1977) structure function methodology. Generally two 76.2 µm diameter thermocouples are used to perform temperature measurements.

The second thermocouple is just a repetition, to take into account possible breaking of one of the two sensors. The thermocouples are mounted at the same height, and temperature was recorded at a frequency of 4 Hz. It seems that it is a sufficient high frequency for sampling over most crops. Typically, time lags of r=0.25 and r=0.50 are used for most canopies. The procedure to compute time lag temperature differences and the statistical moments is described below. If T_4, T_3, T_2 and T_1 are the previous readings, taken at 1.0, 0.75, 0.50 and 0.25 seconds and T_0 is the current temperature, then, before a new datum collection, T_4 is overwritten by T_3, T_3 by T_2, T_2 by T_1, T_1 by the previous T_0 and a new value of T_0 is recorded. This procedure is repeated for both thermocouples. Then, using time lags r=0.25 and r=0.50 the differences (T_1-T_0) and (T_2-T_0) are temporarily stored, then the second, third and fifth moments of these differences are calculated and temporarily stored. At the end of the half hourly period, the means of the 2nd, 3rd and 5th moments are calculated and stored in the output table.

3.3 Eddy covariance theory

The basis of the eddy flux method is to erect a notional control volume over a representative patch of surface, in order to measure the exchange across all the aerial faces of this volume, as well as by recording any accumulation within it, and then to infer the surface exchange by difference. We rely on turbulent mixing to act as a physical averaging operator, so that measurements at some height *h* capture exchange from a representative surface patch. If we assume that, when averaged over sufficiently long time, the flow field is effectively one-dimensional, we can write:

$$\frac{\partial \overline{c}}{\partial t} + \frac{\partial \overline{wc}}{\partial z} = \overline{S}\delta(z) \tag{34}$$

where *c(t)* is a generic scalar, *w(t)* is the vertical component of the velocity vector, the overbar denotes a filtering, detrending or averaging operation, $\overline{S}$ is the surface exchange, *z* the vertical or surface normal coordinate and *δ(z)* is the Dirac delta function. When the flow field is stationary, for example when there is no accumulation of the scalar *c* in the control volume, then the first term of the left side of eq. 34 is zero and thus:

$$\frac{\partial \overline{wc}}{\partial z} = \overline{S}\delta(z) \tag{35}$$

By integrating equation (35) from $z = 0$ to the sensor height h (the top of the control volume) we have:

$$\overline{wc}(h) = \overline{S} \tag{36}$$

The left hand side of equation (36) is the total covariance of $w(t)$ and $c(t)$ under a chosen averaging operator. One final step is required to replace $\overline{wc}(h)$ by the measured eddy flux.

$$\overline{wc} = \overline{\overline{w}\,\overline{c}} + \overline{w'c'} \tag{37}$$

In horizontal homogeneous flows with z-axis normal to the surface, $\overline{w} \to 0$ and the integrated mass balance becomes a statement of the equality of the eddy flux at height h and of the surface exchange. So:

$$\overline{w'c'}(h) = \overline{S} \tag{38}$$

The presented theory explains how the eddy flux is equals to the surface exchange only under a set of quite restrictive conditions. Horizontal homogeneity is necessary if we ignore horizontal flux divergences; stationary is required to ignore storage term, and both coordinate rotation and an averaging operator (that obeys to Reynolds averaging rules) are required to replace the total covariance $\overline{wc}$ by the eddy covariance $\overline{w'c'}$.

4. Materials and methods

Micrometeorological experiments were conducted over orange orchards in the Catania Plain (Eastern Sicily, Italy). Energy balance stations were installed to measure the energy exchange fluxes in the soil-plant-atmosphere continuum. Surface Renewal was the main method for the sensible heat flux estimates. Eddy covariance stations were, also, used to compute the alpha calibration factor for surface renewal and to provide the closure of the energy balance equation.

4.1 Sites description

The experiment was carried out over a 120 ha (37° 16′ 41′′N 14° 53′ 01′′ E) orange orchard located in Lentini (Eastern Sicily, Italy) from September 2009 to September 2010 (Fig. 4). The orchard architecture consisted of mature trees, 3.7 m tall, with a mean leaf area index (LAI) of 4.25 m^2 m^{-2}, PAR light interception of 100% within rows and of 50% between rows. Orange orchards were surface drip irrigated with daily frequency during May-October period. The irrigation systems included on-line labyrinth drippers, in a number of four per plant, spaced at 0.80 m, with discharge rate of 4 l/h at a pressure of 100 kPa.

There was 4 meter of distance between trunks within rows and 5.5 m between rows. The field provides an opportunity for micrometeorological studies because of the flat, homogeneous and wide site. The site is located within the agricultural context of the Catania Plain (Eastern Sicily) where clear skies, high summer temperature, light wind, no rainfall during summer and regional advection were the typical weather conditions. Regardless of the wind direction, the fetch was large because the trees were similar for the adjacent plots.

Fig. 4. Experimental orange orchard at Lentini

The eddy covariance (EC) technique (Aubinet et al. 2000) was used to simultaneously measure the mass and energy exchange flux densities over the orchard field. It encompassed a 3-dimensional sonic anemometer (CSAT3) for measuring the components of wind and a fast-responding open-path gas analyzer LI-7500 (LI-COR, Lincoln, NE, USA) to measure carbon dioxide and latent heat flux. The EC equipment was mounted at 8 meter above the soil surface.

The net radiation (R_n) over the crop (at 8 meter from soil surface) was measured by using two net radiometer (CNR 1 Kippen&Zonen). Net radiation measurements were representative of the average mixed conditions characterizing the heterogeneous context under study. At the plot, soil heat flux (G) was measured using a network of three soil heat flux plates (HFP01, Campbell Scientific Ltd), which were placed horizontally 0.05 meter below soil surface. Three different measurements of G were selected: in the trunk row (shaded area), at 1/3 distance to the adjacent row, and at 2/3 of the distance to the adjacent row. The soil heat flux was measured as the mean output of three soil heat flux plates. The gradual build up of plant matter changed the thermal properties of the upper layers. Consequently, heat storage (ΔS) was quantified in the upper layer by measuring the time rate of change in temperature. The net storage of energy (ΔS) in the soil column was determined from the temperature profile taken above each soil heat flux plate. Three probes (TCAV) were placed in the soil to sample soil temperature. The sensors were placed 0.01-0.04 m (z) below the surface; the volumetric heat capacity of the soil C_v was estimated from the volumetric fractions of minerals (V_m), organic matter (V_0) and volumetric water content (θ). Therefore, G at the surface is estimated by measuring G' at the depth of 0.05 m and the change in temperature with time of the soil layer above the heat flux plates to determine ΔS.

$$G = G' + \Delta S = G' + C_v \left(\frac{T_f - T_i}{t_f - t_i} \right) \cdot d_g \tag{39}$$

where G' is the heat flux density measured by the plate, ΔS is the heat storage, Tf is the final temperature at time tf, Ti is the initial temperature at time ti (the measurement time interval was of 30 min), dg is the depth (m) of the heat flux plates, and Cv is the volumetric heat capacity ($J \cdot m^{-3} \cdot K^{-1}$), which depends on the bulk density (ρb) of the soil and the volumetric water content (θ).

The SR method to estimate H is based on high frequency temperature measurements. When plotted, the temperature traces show ramp like characteristics, which are used to estimate heat fluxes using a conservation of energy equation. Fine-wire thermocouples (76.2 μm dia.)

were, thus, used to measure high frequency (10 Hz) temperature fluctuations. For the experimental site, two thermocouples were mounted 0.5 m above the canopy height and SR estimates of H were computed using a structure function (Van Atta, 1977) and time lags of 0.25 and 0.50 seconds for each thermocouple to determine the mean ramp-like temperature trace characteristics. A 3-D sonic anemometer (Windmaster Pro, Gill Instruments Ltd) was set up at 0.5 meter above the canopy top. The three wind components and air temperature were recorded at 10 Hz. Wind components were rotated to force the mean vertical wind speed to zero and to align the horizontal wind speed to the mean streamwise direction.
Volumetric water content was measured hourly from 0.3 to 0.6 meter below soil surface by using the time domain reflectometry theory (TDR) (CS 616, Campbell Scientific, Logan UT, USA). The site was also equipped with an automatic weather station to measure the values of ancillary meteorological features (i.e. solar radiation, precipitation, air temperature, relative humidity, pressure, wind speed and direction).
Air temperature and wind speed profiles were realized within the orchard in order to apply the aerodynamic analysis. Wind speed and air temperature sensors were installed at 4.5, 6.0, 8.0 and 13.0 meter above the soil surface; data were recorded at 10 minute intervals. To monitor canopy temperature and detect stress conditions onset, five infrared thermometers (IRTS-P, Apogee) were installed within the orchard.
Data gap-filling due to systems stop was performed. In order to take into account of the data gaps, a parametrization was used as outlined in Aubinet et al. (2000) when meteorological data was available. In the case of unavailable data, the missing flux was replaced by interpolation.
The second experimental site is a citrus orchard located in the north-east part of the Catania Plain near Motta Sant'Anastasia (37°29'36"N - 14°55'12"E). The study area has a surface of almost 2.5 ha (200 x 125 m), all around there are citrus orchards divided from little farm road. The experimental field is a fifteen year old orange orchard, the average height of the trees is 4.0 m; plant are spaced 5m x 5m with a density of 400 trees ha^{-1}, and 70% of ground cover (C_g) (Fig. 5).

Fig. 5. Experimental orange orchard at Motta S. Anastasia

The orchard is irrigated by micro-sprinklers system with a flow rate of 140 l/h, working at a pressure of 172 kPa, with a coverage angle of 360°. The irrigation schedule is not regular, and it is decided by the farmer. Usually the irrigation timing is 3-4 hours for each irrigation, which means around 20 mm, every 2 weeks. An energy balance station was installed in the

field to monitor the exchange energy fluxes (net radiation, soil heat flux density, sensible heat flux density and latent heat flux density) in the soil-plant-atmosphere continuum.

Fig. 6. Fine wire thermocouples

The net radiation (R_N, W m^{-2}) was measured using a net radiometer (CNR1, Kipp&Zonen) placed at 1.5 m height above the canopy top. The soil heat flux (G, W m^{-2}) was measured as the mean output of three soil heat flux plates (model HFP-01, Hukseflux Thermal Sensors). They were buried 0.05 m below the surface. The heat storage (ΔS) was quantified in the upper layer by measuring the time rate of change in temperature (Fuchs and Tanner, 1967). Three probes (TCAV) were placed in the soil to sample soil temperature. The sensors were placed 0.01-0.04 m (z) below the surface. In particular the first measurement point was placed near the trunk of the tree (shaded), the second was palced at 1/4 of the distance to the next raw (middle), and the last at 1/2 of the distance to the next raw.
The sensible heat flux density (H) was measured using surface renewal technique. For this pourpose two Campbell's FW3 fine wire type E thermocouple were installed 0.5 m above the top of the canopy (Fig. 6).
The volumetric water content of the soil under study was monitored using 10 Campbell's TDR model CS616 for computing the soil thermal conductivity. Campbell Scientific IRR-P infrared thermometers were installed one meter above the canopy, looking downward to measure the canopy temperature. An infrared temperature sensor is a non-contact probe, that measures the surface temperature of an object by sensing the infrared radiation emitted by the target. The IRR-P is widely used to measure the surface canopy temperature. With contact sensors it's difficult to avoid influencing temperature, maintain thermal contact, and provide a spatial average. By mounting the IRR-P at an appropriate distance it is possible measure the temperature of just one leaf, a canopy or any surface of interest. The canopy temperature is useful for the computation of the Crop Water Stress Index (CWSI), which uses the difference between the canopy temperature and the air temperature to quantify the stress condition of the plant.
The latent heat flux density (LE) was finally computed as residual of the energy balance equation neglecting the small Misc. term. To convert the latent heat flux (LE) into actual water mass flux (ET_a), LE was divided by the latent heat of vaporization (L) equal to 2.45 [MJ kg^{-1}]. Estimates of crop coefficient K_c, obtained as ration between ET_a (assuming ET_a=ET_c due to well watered conditions) and reference ET (ET_0), were compared with K_c data from FAO papers.

Sensible heat flux data from SR technique (H_{SR}) were calibrated with independent measurements of H_{EC} by a 3-D sonic anemometer (Gill Wind-Master) located in the same area of study. The calibration data subset was used to derive the α value by simple linear regression forced through the origin. For this regression, H_{EC} was used as the dependent variable and H_{SR} as the independent one. In this way, the regression slope was the α value looked for, used to correct H from the uncalibrated SR analysis.

4.2 The simplified aerodynamic method

By adopting the micrometeorological aerodynamic method, the sensible heat flux H is determined by the flux-gradient relationship. From the applicative point of view, the main advantage of the aerodynamic method consists in avoiding humidity measurements. Nevertheless, its accuracy depends on the number of measurement levels of wind speed (u) and temperature profile (T).

A simplified version of the method has been proposed by Itier (1981) and Riu (1982). In this version, the measurement of Δu and ΔT is only necessary on two levels. The method is based on the flux-gradient relationship and the Monin-Oboukhov similarity theory. Calculation of H is dependent on atmospheric stability which is estimated by means of the Richardson number, R_i:

$$R_i = \frac{g}{T}\frac{\partial T / \partial z}{\left(\partial u / \partial z\right)^2} \tag{40}$$

where g (m s^{-2}) is the acceleration due to gravity. On the basis of R_i values, H calculation is made by four equations:

i. Moderate instability condition ($-0.3 \le R_i \le 0$, day situation):

$$H = K\Delta T\Delta u\left(1 - K_R\frac{\Delta T}{\Delta u^2}\right)^{3/4} \tag{41}$$

where K e K_R are coefficients depending on the position of the sensors:

ii. Very unstable condition ($Ri < -0.3$, day situation):

$$H = \alpha\Delta T^{3/2} \tag{42}$$

iii. Moderate stability condition ($0 < Ri \le 0.15$, night situation):

$$H = K\Delta T\Delta u\left(1 - \frac{\Delta T\Delta z}{6\Delta u^2}\right)^2 \tag{43}$$

iv. Very stable condition ($Ri > 0.15$, end of clear nights):

$$H = K\frac{\Delta T\Delta u}{10} \tag{44}$$

In the application of the simplified aerodynamic method (SAM) two elements must be underlined: (i) measurements levels z_1 and z_2 must be chosen so that z_2 is high enough to keep $(z_1.z_2)^{1/2}$ outside the roughness layer; (ii) (z_2-z_1) must be large enough to measure wind

and temperature differences with sufficient accuracy. In the proposed application of the method, for the case study of Lentini, z_1 was posed at 4.5 meter and z_2 assumed values of 6, 8 and 13 meters, respectively, from the soil surface layer.

4.3 Performance indicators

Linear regression analysis, L_{RA} (slope, intercept, determination coefficient R^2) and the root mean square error, RMSE, were used to compare the sensible heat flux estimates using SR (H_{SR}) and SAM (H_{SAM}) analyses against the eddy covariance (EC) method (H_{EC}). The coefficient $D=\Sigma y/\Sigma x$ which is the sum of the flux estimates (Σy) over the sum of fluxes taken as reference (Σx), where H_{EC} is the reference data, was also determined as an evaluation parameter. The bias is (D-1) time the mean value determined from the observations. Parameter α of eq. 33 is a factor that corrects the unequal amount of the scalar (T, air temperature) from the measurement height to the ground. If the scalar trace is measured at one height only, α must be determined by comparison of SR results with independently measured exchange rates. In the study, sensible heat flux data from SR technique (H_{SR}) were calibrated with independent measurements of H_{EC} by two 3-D sonic anemometers located, respectivley, at 4 and 8 meters. The calibration data subset was used to derive the α value by simple linear regression forced through the origin. For this regression, H_{EC} was used as the dependent variable and H_{SR} as the independent one. In this way, the regression slope was the α value looked for, used to correct H from the uncalibrated SR analysis.

5. Results and discussion

5.1 The case study of lentini

The values of sensible heat flux (H) estimated from SR and SAM were compared versus the H measured using the EC system deployed at z = 8 m, (i.e., it is the H desired to estimate LE). Figure 7 shows the energy balance closure at 8 meter. The H values estimated from SR and SAM (with z_2=13 meter) were close to H from EC method. Figures 8 and 9 show that the hourly H_{SR} and H_{SAM} versus H_{EC} were similar for a wide range of H. When the simplified aerodynamic method (SAM) was applied with z_2 at 8 or 6 meter, H_{SAM} resulted quite different from H_{EC}. Most likely (z_2-z_1) wasn't large enough to measure wind and temperature differences with sufficient accuracy. In fact, when the atmospheric surface boundary layer is moderate or quite unstable, similar studies indicate that the roughness sub-layer depth mostly varies from 1 to 2 times the canopy height (Castellvì and Snyder 2009). Fig. 10 shows the frequency of z = 8 m to be above the roughness sublayer versus time (GMT).

In general, it is shown that for hours with negative (Rn-G), the measurement height mainly remained within the inertial sub-layer. For positive (Rn-G) the roughness sublayer depth was oscillating around the upper level for about the 50% of the samples from sunrise until about two hours after noon, and during late afternoon the upper level tended to remain in the inertial sublayer.

Furthermore, some spurious H estimates were obtained from SAM during moderate and very stable atmospheric conditions, thus reducing the available data set for the comparison. In particular, the number of samples gathered under unstable atmospheric conditions was higher than that from stable conditions.

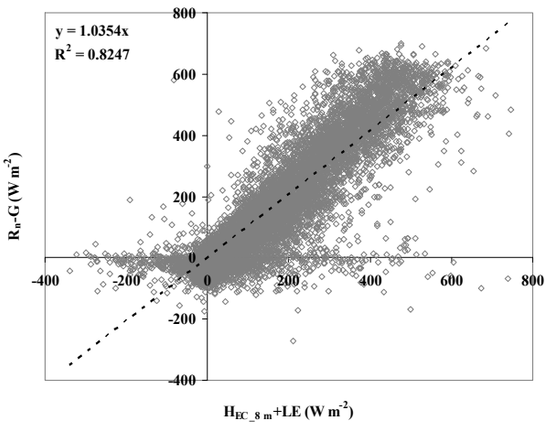

Fig. 7. Energy balance closure at 8 meter

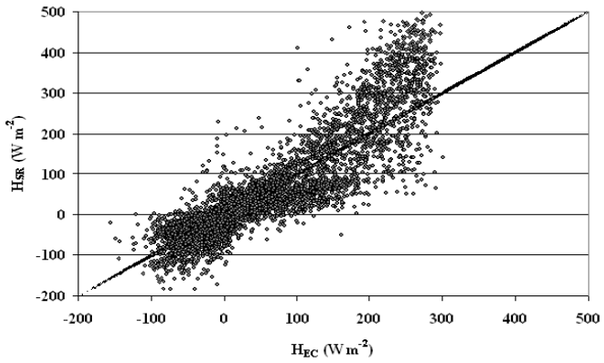

Fig. 8. H_{SR} versus H_{EC} at 8 meter

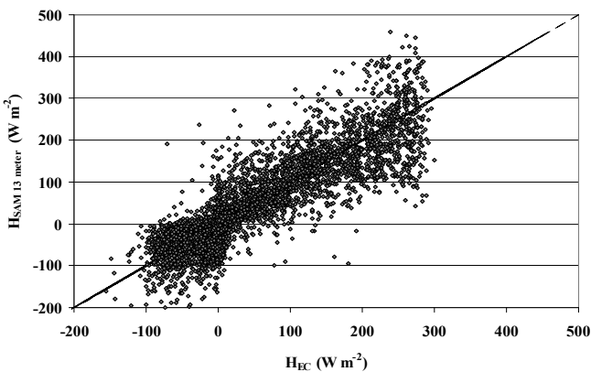

Fig. 9. H_{SAM} at 13 meter versus H_{EC} at 8 meter

Table 1 shows the results of the linear regression analysis (slope, intercept and coefficient of determination, R^2), root square mean error, RMSE, and D obtained for the analyzed data set. The largest RMSE values were obtained using the simplified aerodynamic method applied at 8 and 6 meters.

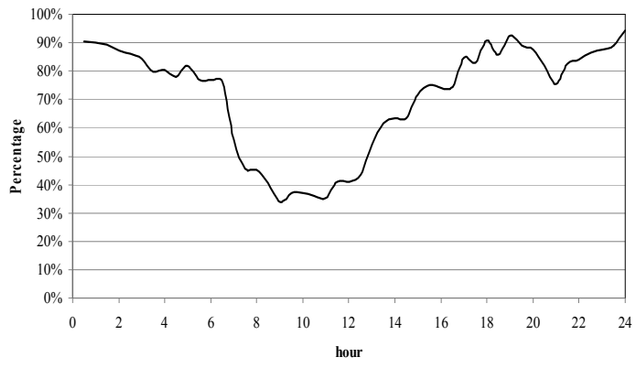

Fig. 10. Percentage of cases when z=8 m falls above z*

In a review of experiments where the measurements were taken in the roughness sublayer, the RMSE values found to adjust surface renewal method where lower than that in Table 1 (Paw U et al. 1995; 2005). However these experiments are not direclty comparable because H was measured using a one dimensional sonic anemometer.

Slight underestimations by the proposed alternative methods (SR and SAM) were observed. A 3.8% underestimation was found by SR for the whole data set including both stable and unstable cases; as a result that for small fluxes the ramp amplitude was often not in accord with the sign of $H_{EC.}$ RMSE values from SR and SAM were not high. SR and SAM linear regression analyses showed slopes of, respectively, 1.12 and 0.95 very close to unit, intercepts near zero and high coefficients of determination.

For optimized drip irrigation, hourly LE estimates are desired. The best LE estimates from eq.2 are attained when all the terms are averaged hourly. A better closure may be achieved when turbulent fluxes are determined using longer block averages than half-hourly because lower frequencies are captured as well (Finningan et al. 2003). However, SR is based on the analysis of organized motion near the canopy-atmosphere interface. The continuous ramp patter exhibited in the scalar trace is a canopy-scale coherent structure, which is not associated with large circulations.

	H_{SR} versus H_{EC}	H_{SAM} (z_2= 13 m) versus H_{EC}	H_{SAM} (z_2= 8 m) versus H_{EC}	H_{SAM} (z_2= 6 m) versus H_{EC}
A	1.12	0.95	1.20	1.87
b (W m^{-2})	-5.80	-2.33	2.96	-4.58
R^2	0.80	0.77	0.63	0.75
RMSE (W m^{-2})	50.19	44.52	58.92	117.11
D	0.96	0.88	1.11	1.72

Table 1. Linear regression analysis, RMSE, D and, comparing the hourly H_{SR} and H_{SAM} (with different z_2) versus H_{EC} for the whole data set.

During the irrigation season (May-October period), latent heat flux density averaged 8.5, 7.0, and 7.6 MJ m^{-2} d^{-1} for the EC, SR and SAM, respectively. The mean (about 0.90) of daytime evaporative fraction (EF) during summer, which characterizes the partition of the energy budget at the daily time scale, varied little (0.06) based on average cloudiness. The temporal variability of the partitioning, expressed in terms of EF daily standard deviation, reached a

maximum of 14%. The experiment showed that the evaporative fraction computed from flux measurements at 4 hours past sunrise tends to increase very slowly, thus to assume that the underestimation in daytime average would be not significant. Actual crop ET (ET_a) was computed by dividing LE by the latent heat of vaporization: L = 2.45 MJ m^{-2} mm^{-1}. Generally, crop coefficients are determined by calculating the ratio $K_{co}=ET_c/ET_o$, where ET_c is the evapotranspiration of a well-watered crop. Since these orchards are well managed, it is assumed that there was little or no transpiration reducing water stress and $ET_a \approx ET_c$.

Hourly variations of crop coefficient (K_{co}) values, during the monitoring period, were determined using ET_c and reference evapotranspiration (ET_o) for a short canopy (Allen et al. 1998). Weather data used to calculate ET_o came from the SIAS station (the agro-meteorological service of the Sicilian region) which is located 4 km far from the site. Hourly ET_o values were summed over 24-hour periods to obtain daily ET_o.

During May-October period, average daily values of ET_c were of 3.5, 2.9 and 3.1 respectively from EC, SR and SAM, with corresponding values of crop coefficient of 0.54, 0.51, and 0.62.

H_{EC_4m} and H_{EC_8m} were rather well correlated (R^2=0.93) considering the different amount of small eddies (much higher close to the canopy top) that cannot be properly sampled by sonic anemometer. Figure 11 shows H_{EC_4m} versus H_{EC_8m} for all the campaign. In general H_{EC_4m} underestimated H_{EC_8m} of 18%. For unstable cases, the α values for unequal heating was of 0.66 at 4 meter and of 0.68 at 8 meter.

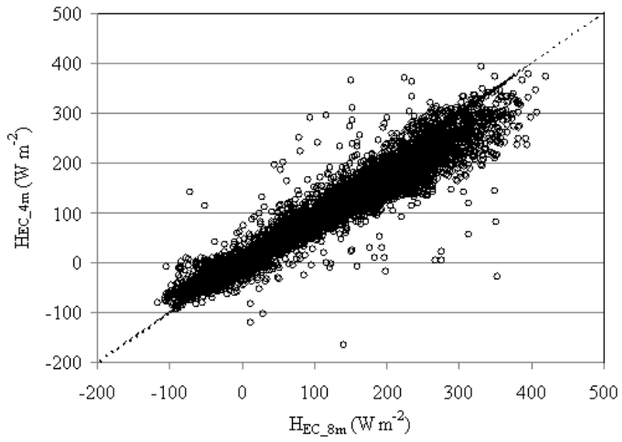

Fig. 11. Sensible heat flux measurements using the EC method at z=4 m, H_{EC_4m} versus at z=8 m, H_{EC_8m} for all the data.

5.2 The case study of Motta S. Anastasia

Table 2 shows the mean values for surface fluxes corresponding to four different datasets during the monitoring periods. Two datasets were formed from samples gathered under unstable and stable surface-layer atmospheric conditions. In particular, stable-case data set corresponded to night time periods with negative R_N-G (available energy) and small H and LE. The unstable data set is referred to diurnal periods where R_N-G is positive, with the exception of the periods close to sunrise, sunset and late afternoon that may be included in the stable-case data set. The dry and humid period data sets correspond, for the area under study, to May-September and October-April, respectively.

Year	atmospheric condition		H_{SR} (W m^{-2})	LE (W m^{-2})	R_N-G (W m^{-2})
2005	unstable	Dry period	77.4	255.8	331.6
		Humid period	27.9	116.1	143.8
	stable	Dry period	-11.9	-32.6	-45.2
		Humid period	-18.7	-23.7	-42.0
2006	unstable	Dry period	34.9	283.5	320.3
		Humid period	35.2	140.0	176.9
	stable	Dry period	-4.6	-29.4	-35.9
		Humid period	-10.5	-28.5	-39.6
2007	unstable	Dry period	34.6	262.9	299.6
		Humid period	19.4	157.0	177.8
	stable	Dry period	-4.4	-30.2	-36.5
		humid period	-6.4	-28.6	-36.0
2008	unstable	Dry period	77.5	146.0	223.6
		humid period	42.6	108.5	151.0
	stable	Dry period	-4.9	-29.7	-36.9
		humid period	-8.8	-24.7	-33.9

Table 2. Mean values of energy fluxes during unstable and stable conditions

As shown in Table 2, the energy partitioning of the available net surface energy was remarkably distinct for these different datasets. During both dry and humid periods well-formed ramp traces of air temperature were observed, which explains the good performance of LE values. Under unstable atmospheric conditions, when a cool air parcel moves instantaneously downward and travels horizontally, a positive amplitude ramp (a) in the temperature trace is observed (positive H). For this reason, in the unstable-case when RN-G is positive, most of the available net surface energy contributes to positive latent heat flux. It reached a maximum of around 650 W m-2 during late July of the monitoring periods. The average hourly ratio H/LE during dry periods was around 0.56 and reached the peak between 12.00 a.m. and 2.00 p.m. Under stable atmospheric conditions, the temperature, generally, risen as the warm air swept into the canopy an heat transferred from the air to the plant canopy elements, causing a slow temperature drop ($a<0$ and $H<0$). In the study, the latent heat flux, the energy transfer due to evaporation or condensation, was largely dependent on leaf area index (LAI) and PAR light interception (LI) by vegetation, with peaks when LAI and PAR LI were higher.

The hourly patterns of energy fluxes in the orchard is presented for the same days-period in Figure 12. In all the years the energy balance calculations were fairly similar. On the average, the evaporative fraction EF (%), the ration between LE and the available surface energy (R_N-G) was of about 80%, during the dry period and under unstable-case atmospheric conditions.

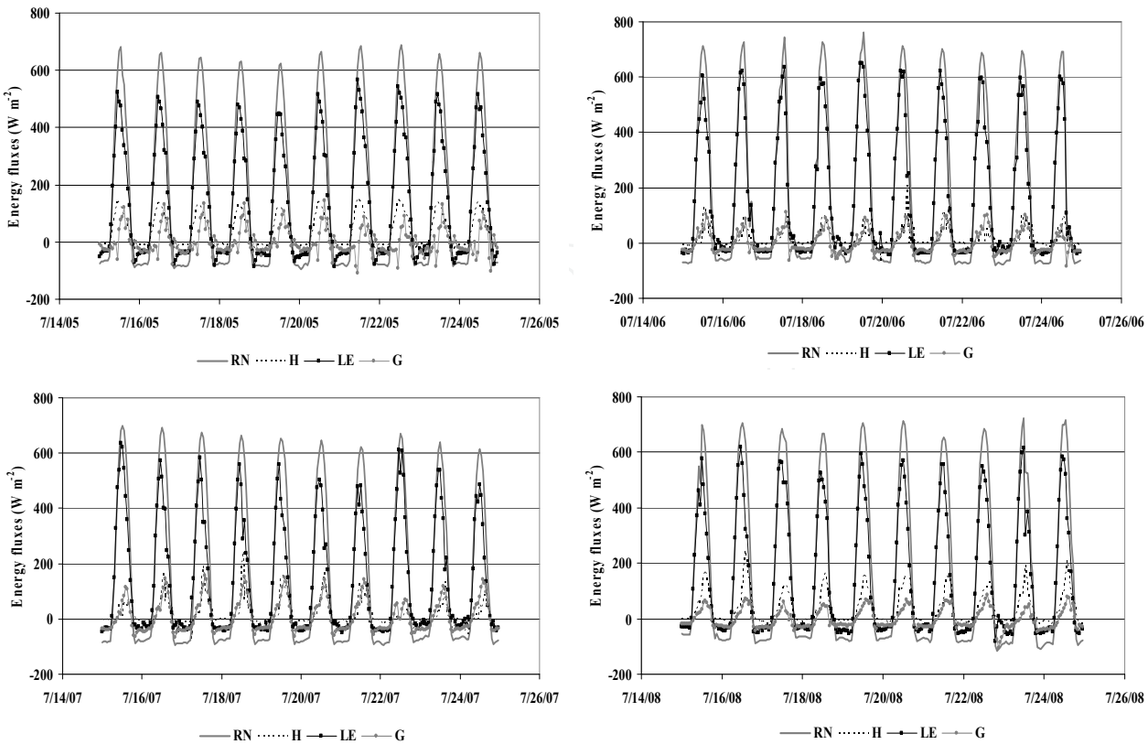

Fig. 12. Hourly patters of energy fluxes in the orchard for 10-days periods during the monitoring years

The regression of half hourly averages of sensible heat flux density (H_{EC}) from the sonic anemometer versus uncalibrated Surface Renewal measurements of H was carried out during the months of July of the years 2005 and 2006. The slope of the regression of H_{EC} versus uncalibrated H_{SR} was of about 0.24 with a determination coefficient R^2=0.85. This calibration for α was used during 2007 and 2008.

During summer, LE values had an average of about 11.0 MJ m^{-2} d^{-1} and a maximum of 17.4 MJ m^{-2} d^{-1}, with a variation of about 0.5. Study revealed that net radiation (R_N) was highest at 12.00 noon, with the daily mean value of about 13.2 MJ m^{-2} d^{-1}, maximum around 18.0 MJ m^{-2} d^{-1} and variation coefficient of 0.55. The course of soil heat flux (G) was affected by the development of crop canopy or leaf area index. On a daily basis, G density is generally close to zero. Sensible heat flux (H) had mean and maximum values of about 2.2 MJ m^{-2} d^{-1} and 4.7 MJ m^{-2} d^{-1}, respectively; daily H values resulted fairly scattered around the mean, with a variation of about 0.8.

In general, mean reference evapotranspiration ET_0 during dry periods tends to be between 5-6 mm d^{-1} in each year; ET_0 varied between a maximum of about 11 mm d^{-1} to a minimum of about 1.5 mm d^{-1}. The mean ET_a was about 4.5 mm d^{-1} (variation less than 10%) during the dry periods of the monitoring years. Before the experiment in 2005, the orchard was topped and pruned, which probably explains the slightly lower ET_a during that season. During humid periods, mean ET_0 and ET_a were of about 2.3 and 1.8 mm d^{-1}, respectively. Crop coefficient (K_c) values were higher than typical reported (Allen et al., 1998). The K_c values generally increased during the monitored dry periods with averages

of 0.76, 0.89, 0.86 and 0.73 going from 2005 to 2008. In 2005, the increase in summer was due to the canopy growth following topping and pruning. In 2008, the experimental orchard was less vigorous than in the previous years due to a pathogenic diseases caused by the *Closterovirus Citrus Tristeza Virus* (CTV). It determined significant economical income reductions for the grower. The *virus* mainly affects the plant root system and its water supplying capacity; others evident effects concern the reduction of vegetation indicators such as LAI, WDVI, NDVI and PAR light interception by the monitored orchards.

The rows at the experimental orchard are east-west oriented rather than north-south and this might partially explain the higher crop coefficient values. Another possible reason for the higher K_c values observed in this experiment is the use of micro-sprayer irrigation rather than surface irrigation and higher application frequency in this orchard than reported in old experiments (Allen et al., 1998). In fact, these publications do not site the original source of information, and it is likely that the values came from research on flood or furrow irrigated citrus orchards prior to 1977, so those data may be too low for dense canopy, vigorous, sprayer-irrigated orchards. In the experimental orchard, mean K_c values varied from about 0.83 to 0.74 from June to September of the monitored years. In the widely used FAO papers (27 and 56), the estimated crop coefficient for clean-cultivated, mature (> 70% cover) citrus is given as K_c=0.65 for June through August. Nearly linear relationships between K_c value and LAI and PAR light interception were observed in the study. The peak K_c value occurred at LAI of 1.8 m^2 m^{-2} and PAR light interception of 80%.

6. Conclusions

This chapter gives the micrometeorological basics, which were applied in the presented experimental researches. The energy balance equation and the principal micrometerological methods to estimate its flux components were presented. The reliability of alternative micrometerological techniques, such as Surface Renewal for estimating sensible heat fluxes was proposed and discussed. Two different study cases were presented both realized within a Mediterranean environment, characterized by semi-arid climatic conditions and water availability restrictions for agricultural purposes. On the basis of the first experimental results, carried out within the orange orchard located in Lentini (Eastern Sicily), two alternative methods: Surface Renewal (SR) and a simplified aerodynamic method (SAM) for estimating sensible heat fluxes were proposed and compared with the more rigorous eddy covariance technique at the same site. The SAM analysis was accomplished by coupling different equations based on simple gradient flux expressions to account for atmospheric changes depending on stability or unstability conditions. In general H_{SR} and H_{SAM} were similar to H_{EC} regardless of the atmospheric stability conditions, demonstrating the potential of SR and SAM analyses as methods applicable to estimate sensible heat flux. The SAM was more sensitive to moderate and very stable atmospheric conditions, thus resulting in some spurious data. SR technique appears in advantage with respect to SAM and EC because it may operate close to the canopy, thus minimizing fetch requirements, which make it a useful micrometeorological method where fetch requirements limit the application of other techniques. The combination of the SR procedure and the simplified surface energy

balance equation appears to be an affordable alternative to be considered for estimating water use in agriculture.

According to the second experiment, data were collected over orange orchards and analyzed for different ranges available energy, sensible and latent heat fluxes during the monitoring period 2005-2008 in Motta S. Anastasia (Eastern Sicily). During unstable atmospheric conditions, the surface energy balance analysis revealed hourly sensible heat fluxes similar to soil heat flux data, with a mean partitioning of available energy into latent heat flux of about 80%. The crop coefficient (Kc) shows apparent correspondence with the development of canopy cover, LAI and PAR Light interception. The established relationships can be useful for development algorithm of crop simulation model for predicting LAI or PAR LI. Crop coefficient values estimated from the field experiment during 2005-2008 monitoring periods were quite different (means between 0.73 and 0.89) from the crop coefficients published by FAO (0.65) for citrus with ground cover by vegetation of about 70%. Differences between observed Kc and old Kc values from FAO papers are most likely due to differences in plant density, cultural practices, irrigation methods (micro irrigation techniques versus surface irrigation) and frequencies and methods to estimate references ET rates.

To conclude, measurements of high frequency temperature data for the case study showed that the structure function approach used in Surface Renewal analysis provide a good performance in terms of both H and LE. Fairly high correlation were found between calibrated Surface Renewal H_{SR} and Eddy Covariance H_{EC} (from sonic anemometer). By working at 4 Hz, Surface Renewal uses a smaller amount of data than Eddy Covariance (10 Hz) and allows an easier and cheap computation of sensible heat fluxes.

7. References

Allen, R. G.; Pereira, L. S., Raes, D. & Smith M. (1998). Crop evapotranspiration: Guidelines for computing crop water requirements. Irr. & Drain. Paper 56, FAO Rome

Aubinet MA; Grelle A. & Ibron. A (2000). Estimates of the annual net carbon and water exchange of forests: the EUROFLUX methodology. *Adv. Ecol. Res.,* Vol.30, pp. 113–175

Castellvi F.,; Snyder R.L. & Baldocchi D.D. (2008). Surface energy-balance closure over rangeland grass using the eddy covariance method and surface renewal analysis. *Agric. For. Meteorol.,* Vol.148 No.6-7, pp. 1147-1160

Castellvì F. & Snyder R.L. (2009). On the performance of surface renewal analysis to estimate sensible heat flux over two growing rice fields under the influence of regional advection. *J. Hydrol.,* Vol.375, pp. 546-553

Chen, W.,; Novak, M. D., Blanck, A. & Lee, X. (1997). Coherent eddies and temperature structure functions fro three contrasting surfaces - Part I: ramp model with finite microfront time. *Bondary-Layer Meteorol*. Vol. 66, No 1-2, pp. 65-80

Consoli, S.,; O'Connell, N.V. & Snyder, R.L. (2006). Estimation of evapotranspiration of different orange sized orchard canopies using energy balance. *J. Irr. and Drain. Engineer.* ASCE. Vol. 32, No 1, pp. 2-8

Desjardins, R.L. (1972). CO2 measurements by eddy correlation methods. *Bulletin of the American Meteorological Society*, Vol. 53, pp. 10-40.

Finnigan, J.J.,; Clements, R., Malhi, Y., Leuning, R. & Cleugh, H. (2003). A revaluation of long-term flux measurement techniques. Part I: averaging and coordinate rotation, *Boundary-Layer Meteorology,* Vol.107, pp. 1-48

Gao, W.,; Shaw, R.H. & Paw U, K.T. (1989). Observation of organized structure in turbulent flow within and above a forest canopy. *Bounday-Layer Meteorology,* Vol. 47, pp. 349-377

Itier, B. (1981). Une mèthode simple pour la mésure du l'evapotranspiration réelle à l'échelle de la parcelle, *Agronomie,* Vol.1, pp. 869-876

Paw U, K. T. & Brunet, Y. (1991). A surface renewal measure of sensible heat flux density. *In preprints, 20th Conference on Agricultural and Forest Meteorology*, pp. 52-53, Salt Lake City, Utah, September 10-13

Paw U, K.T.,; Brunet, Y., Collineau, S., Shaw, R.H., Mitani, T., Qui, J. & Hipps, L. (1992). On coherent structures in turbulence within and above agricultural plant canopies. *Agricultural and Forest Meteorology*, Vol. 61, pp. 55-68

Paw U, K. T.,; Qui, J., Su, H. B., Watanabe, T. & Brunet, Y. (1995). Surface renewal analysis: a new method to obtain scalar fluxes without velocity data. *Agric. For. Meteorol.* Vol. 74, pp. 119-137

Paw U, K.T., Baldocchi, D.D., Meyers T.P. & Wilson, K. (2000). Correction of eddy-covariance measurements incorporating both the advective effects and density fluxes. *Boundary-Layer Meteorology*, Vol. 97, pp. 487-511

Pruitt, W.O. (1963). Application of several energy balance and aerodynamic evaporation equations under a wide range of stability. *Final Report to USAEPG on contract no. DA-36-039-SC80334*. University of California, Davis (Ed.), pp 107-124

Riou, C. (1982). Une expression analytique du flux de chaleur sensible en conditions superadiabatiques à partir de mesures du vent et de la témperature à deux niveux. *J. Rech. Atmos.*, Vol. 16, pp. 15-22

Snyder, R.L.,; Spano, D. & Paw U, K.T. (1996) Surface Renewal analysis for sensible and latent heat flux density. *Boundary-Layer Meteorol*., Vol. 77, pp. 249-266

Snyder, R.L.,; Bali, K., Ventura, F. & Gomes-MacPherson H. (2000). Estimating evapotranspiration from bare soil or nearly bare soil. *J. Irrig. & Drain. Eng*., Vol.126 No(6), pp. 399-403

Spano D.,; Snyder, R.L., Duce, P. & Paw U, K.T. (1997). Surface renewal analysis for sensible heat flux density using structure functions. *Agric. For. Meteorol.* Vol. 86, pp. 259 - 271

Stull, R.B. (1984). Transilient turbulence theory. 1. The concept of eddy-mixing across finite distances. *Journal of Atmospheric Science,* Vol.41, pp. 3351-3367

Stull, R.B. (1988). *An Introduction to Boundary Layer Meteorology*, Kluwer Academic Publishers.

Swinbank, W.C. (1955). *Eddy transport in the lower atmosphere*. Technical paper No.2, Division of Meteorological Physics, Commonwealth Scientific and Industrial Research Organization, Melbourne, Australia. 30pp

Tillman, J. E. (1972). The Indirect Determination of Stability, Heat and Momentum Fluxes in the Atmospheric Boundary Layer from Simple Scalar Variables during Dry Unstable Conditions. *Journal of Applied Meteorology*, Vol.11, pp. 783–793.

Van Atta, C.W. (1977). Effect of coherent structures on structure functions of temperature in the atmospheric boundary layer. *Arch. of Mech.,* Vol.29, pp. 161-171

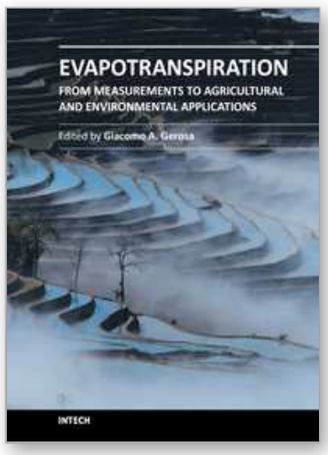

Evapotranspiration - From Measurements to Agricultural and Environmental Applications
Edited by Dr. Giacomo Gerosa

ISBN 978-953-307-512-9
Hard cover, 410 pages
Publisher InTech
Published online 09, November, 2011
Published in print edition November, 2011

This book represents an overview of the direct measurement techniques of evapotranspiration with related applications to the water use optimization in the agricultural practice and to the ecosystems study. Different measuring techniques at leaf level (porometry), plant-level (sap-flow, lysimetry) and agro-ecosystem level (Surface Renewal, Eddy Covariance, Multi layer BREB), are presented with detailed explanations and examples. For the optimization of the water use in agriculture, detailed measurements on transpiration demands of crops and different cultivars, as well as results of different irrigation schemes and techniques (i.e. subsurface drip) in semi-arid areas for open-field, greenhouse and potted grown plants are presented. Aspects on ET of crops in saline environments, effects of ET on groundwater quality in xeric environments as well as the application of ET to climatic classification are also depicted. The book provides an excellent overview for both, researchers and student,s who intend to address these issues.

How to reference
In order to correctly reference this scholarly work, feel free to copy and paste the following:

Simona Consoli (2011). Evapotranspiration Estimation Using Micrometeorological Techniques, Evapotranspiration - From Measurements to Agricultural and Environmental Applications, Dr. Giacomo Gerosa (Ed.), ISBN: 978-953-307-512-9, InTech, Available from: http://www.intechopen.com/books/evapotranspiration-from-measurements-to-agricultural-and-environmental-applications/evapotranspiration-estimation-using-micrometeorological-techniques

INTECH
open science | open minds

InTech Europe
University Campus STeP Ri
Slavka Krautzeka 83/A
51000 Rijeka, Croatia
Phone: +385 (51) 770 447
Fax: +385 (51) 686 166
www.intechopen.com

InTech China
Unit 405, Office Block, Hotel Equatorial Shanghai
No.65, Yan An Road (West), Shanghai, 200040, China
中国上海市延安西路65号上海国际贵都大饭店办公楼405单元
Phone: +86-21-62489820
Fax: +86-21-62489821

IntechOpen